Preprints (www.preprints.org) | NOT PEER-REVIEWED | Posted: 24 May 2019 doi:10.20944/preprints201905.0301.v1

Peer-reviewed version available at *Appl. Sci.* **2019**, *9*, 2240; doi:10.3390/app9112240

Article

The Antifungal Potential of Carvacrol against *Penicillium Digitatum* through ^{1}H-NMR Based Metabolomics approach

Chunpeng Wan [1], Yuting Shen [1], Muhammad Farrukh Nisar [1,#], Wenwen Qi [1], Chuying Chen [1,*] and Jinyin Chen [1,2,*]

[1] Collaborative Innovation Center of Post-harvest Key Technology and Quality Safety of Fruits and Vegetables in Jiangxi Province, Jiangxi Key Laboratory for Postharvest Technology and Non-destructive Testing of Fruits & Vegetables, Jiangxi Agricultural University, Nanchang 330045, China; chunpengwan@jxau.edu.cn (C.W.); ytshenchina@126.com (Y.S.); farrukh.nisar@hotmail.com (M.N.); qwwbaobei@163.com (W.Q.)

[2] Pingxiang University, Pingxiang Jiangxi 337055, China;

* Correspondence: cy.chen@jxau.edu.cn (C.C.); jinyinchen@126.com (J.C.); Tel.: +86-791-8381-3158 (C.C. & J.C.)

[#] Current Address: Department of Physiology and Biochemistry, Cholistan University of Veterinary and Animal Sciences (CUVAS), Bahawalpur, 63100, Pakistan.

Abstract: Carvacrol (5-Isopropyl-2-methylphenol), a volatile oil constituent, mainly exists in Labiaceae family plants. Carvacrol has long been studied for its natural antifungal potential and food preservative potential. However, its exact mode of action, especially against *Penicillium digitatum* (*P. digitatum*), remains unexplored. Herein, a ^{1}H-NMR-based metabolomic technique was used to investigate the antifungal mechanism of carvacrol against *P. digitatum*. The metabolomic profiling data showed that alanine, aspartate, glutamate, and glutathione metabolism were imbalanced in the fungal hyphae. A strong positive correlation was seen between aspartate, glutamate, alanine, and glutamine, with a negative correlation among glutathione and lactate. These metabolic changes revealed that carvacrol-induced oxidative stress had disturbed the energy production and amino acid metabolism of *P. digitatum*. The current study will improve the understanding of the metabolic changes posed by plant-based fungicides in order to control citrus fruit green mold caused by *P. digitatum*. Moreover, the study will provide a certain experimental and theoretical basis for the development of novel citrus fruit preservatives.

Keywords: amino acid metabolism; carvacrol; metabolomics data; oxidative stress; *Penicillium digitatum*

1. Introduction

Rotting of fruits and vegetables have been a frequent and serious problem for thousands of years. Even in developed countries, the citrus yield loss reaches up to 25%, with developing countries facing almost double this yield loss of citrus crop. This yield loss is causing serious annual economic losses and creating hurdles for the development of the citrus fruits-related industry [1]. Citrus fruits (Family Rutaceae, subfamily Aurantioideae) are highly susceptible to decay caused by more than 20 postharvest fungal infections leading, to approximately half the crop wasted due to fungal diseases [2]. Among various fungal strains, *Penicillium* fungi cause serious plant diseases and damage to the citrus crop during storage, accounting for about 10–30% [3]. The *P. digitatum* infects the citrus fruits, causes green mold disease, and generates huge (60–80%) yield losses under ambient conditions [4]. In order to control such fungal disease-mediated yield losses, prochloraz, imazalil, and thiabendazole are extensively used as potential antifungal agents [5]. The literature reported serious health issues aroused by excessive use of certain routine and synthetic antifungal agents.

© 2019 by the author(s). Distributed under a Creative Commons CC BY license.

Preprints (www.preprints.org) | NOT PEER-REVIEWED | Posted: 24 May 2019 doi:10.20944/preprints201905.0301.v1

Peer-reviewed version available at Appl. Sci. 2019, 9, 2240; doi:10.3390/app9112240

Over the past few decades, the intentions have been to ensure the hygiene and safety levels of fruit products along with promoting maximum biodegradability. In order to achieve this ambition, researchers are still trying to screen natural products with strong antifungal potential from plants. Moreover, it has also been tried to explore new preservation technologies that can replace synthetic fungicides. Compared with synthetic fungicides, natural antifungal substances have attained much attention in recent years [6–9].

Various essential oils refined from *Melaleuca alternifolia* have strong inhibitory effects on multiple fungal strains, particularly *P. italicum* Wehmer and *P. digitatum* Sacc., and hence can be used as natural preservatives in agricultural and food processing [10]. Previously we have reported that cinnamaldehyde contained in cinnamon has a good antifungal effect against *P. italicum* and clarifies the method for dynamic detection of the antifungal effect of cinnamaldehyde [11]. In addition, GC-MS and GC-FID techniques successfully separated the essential oils components *viz*. limonene (87.02%), linalyl acetate (53.76%) and linalool (39.74%) from peels, leaves and flowers of *Citrus aurantium* var amara, neroli oil appeared as the best fungistatic agent, which reduced the *P. digitatum* sporulation to 25 % at a 50 mg/mL concentration of oil [12].

Carvacrol (5-Isopropyl-2-methylphenol) is the major volatile oil constituent from Labiaceae family plants, such as oregano, mint, and thyme [13]. Carvacrol has many medicinal and edible applications, including antifungal, antimicrobial, anti-inflammatory, insecticidal, antitumor, and other effects [14]. Carvacrol inhibited the growth of *P. digitatum* and *P. italicum* in in vitro and in vivo experiments of lemon [15]. Another study in Morocco, reported that *Thymus leptobotrys* and *T. riatarum* have carvacrol contents of 76.94% and 32.24%, respectively, and the former species has the highest bioactivity among the tested plant species in that study. In addition, the study reported a complete inhibition of germination of the spore of *P. digitatum* and *P. italicum* at 500 μL/L [16]. The results of the antimicrobial activity assay showed that carvacrol, cinnamaldehyde, and *trans*-cinnamaldehyde significantly reduced the growth of *P. digitatum*; particularly, the carviniol appeared as the most effective remedy to control *P. digitatum* [17].

Metabolomics is an important part of systems biology, which is quite similar to genomics and proteomics [18]. Metabolomics is distinguished from other related sciences in terms if its ability to find the relative relationship of metabolites with physiological and pathological changes through quantitative analyses of metabolites with low molecular weight (1000) [19]. Recently, the ^{1}H-NMR based metabolomics approach was used to reveal the antimicrobial mechanism, which generally includes amino acid biosynthesis and energy-associated metabolism [20,21]. Although carvacrol already been proved to have significant antifungal properties, the underlying mechanism is not clear yet. In the current study, we applied the ^{1}H-NMR-based metabolomics approach to evaluate the antifungal potential of carvacrol on *P. digitatum* and explored the underlying antifungal mechanism. Moreover, how carvacrol-induced oxidative stress disturbs the energy production and amino acid metabolism in *P. digitatum* shall also be studied through metabolic profiles.

2. Materials and Methods

2.1. Chemicals

Carvacrol (purity 99%) purchased from Shanghai Aladdin Co., Ltd. (C804847), and because of its insolubility in water, it was previously dissolved in ethanol (50%, *w/w*) to obtain a stock solution with a proper concentration of 10 mg·mL^{-1}.

2.2. Preparation of P. Digitatum Spores

The highly pathogenic fungus *P. digitatum* was isolated from an infected orange with typical green mold symptoms and maintained on potato dextrose agar (PDA: 200 g peeled potatoes, 20 g glucose, 18 g agar powder and 1 L distilled water) medium plates at 25 °C. The preparation of *P. digitatum* spore suspension was based on a previous method [22], and the tested pathogen was incubated at 25 °C for 7 days. The seven-days-old plate was washed with sterile water and then gently dispersed by spread bacteria beads to release spores. Finally, the spore suspensions were

Preprints (www.preprints.org) | NOT PEER-REVIEWED | Posted: 24 May 2019 doi:10.20944/preprints201905.0301.v1

Peer-reviewed version available at Appl. Sci. 2019, 9, 2240; doi:10.3390/app9112240

filtered through a sterile cotton ball in a funnel to remove mycelia and PDA fragments and adjusted to the suitable concentration of 1×10^6 spores mL^{-1} with the aid of a hemocytometer.

2.3. Antifungal Effects of Carvacrol against *P.* Digitatum

The inhibitory effect of carvacrol on the mycelial growth of *P. digitatum* was determined as previously reported [22]. Briefly, the 0, 0.0625, 0.125, 0.25, 0.5, and 1 mL of carvacrol stock solution was diluted with 2, 1.9375, 1.875, 1.75, 1.5, 1 mL of sterile 0.5% Tween 80 and mixed with 18 mL of PDA for obtaining the final concentrations of 0 (control), 0.03125, 0.0625, 0.125, 0.25, and 0.5 $mg{\cdot}mL^{-1}$. The mycelial disks (5 mm in diameter), cut from the periphery of a seven-days-old culture using a stainless-steel punch, was placed in the center of each Petri dish (90 mm in diameter). Then, all plates were incubated at 25 °C for seven days. Four replicates were used per treatment and the experiment was carried out at two separate times. Mycelial growth inhibition (MGI) of carvacrol treatment against control was calculated using the following equation:

$$\text{MGI (\%)} = \frac{Dc - Dt}{Dc - 5} \times 100$$

where *Dc* and *Dt* were the mean colony diameter of control and treated sets, respectively.

The minimum inhibitory concentration (MIC) was defined as the lowest carvacrol concentration that completely inhibited the growth of *P. digitatum* after 48 h of incubation at 25 °C. The minimum fungicidal concentration (MFC) was considered the lowest concentration of carvacrol with no visible fungal growth on a PDA plate after a following 5 days incubation at 25 °C [22].

2.4. The Effect of Carvacrol on Mycelial Weights and Water-Retention Rate

The effects of carvacrol on the wet and dry weights as well as the water-retention rate of *P. digitatum* mycelial were determined by the method described by Tian et al. with some modifications [23]. Briefly, 100 μL of *P. digitatum* containing 10^6 spores mL^{-1} was inoculated into 50 mL of potato dextrose broth (PDB) medium and then was incubated in a rotary shaker (150 rpm) at 25 °C. After shake incubating for 48 h, the carvacrol solution at final concentrations of 0 (control), 0.03125, 0.0625, 0.125, 0.25 and 0.5 $mg{\cdot}mL^{-1}$ were added into the above-mentioned PDB and then incubated for 24 h at 25 °C in a rotary shaker. The mycelia from the carvacrol treated and control PDB was collected by filtering used a Buchner funnel and washed three times with sterile water. The wet weights of the mycelia were measured, the mycelia were dried at 70 °C for 12 h, and the dry weights were then measured using an analytical balance (Ms105, Mettler Toledo, Greifensee, Switzerland). The water-retention rates of the carvacrol-treated and control groups were calculated using the following equation:

$$\text{Water-retention rate (\%)} = \frac{Ww - Wd}{Ww} \times 100$$

where *Ww* and *Wd* were the mean of wet and dry weights in carvacrol treated and control sets, respectively.

2.5. Sample Preparation for ^{1}H NMR Spectroscopy

The collected mycelial treated with MIC carvacrol for 4, 8 and 12 h respectively were washed three times with pre-cooled PBS buffer solution and then added with 3.8 mL pre-cooled methanol-water mixture (1/0.9, v/v). The mixture was placed on the ice for 4 min of sonication bathing, and then added with 4 mL trichloromethane. After full oscillation, the mixture was centrifuged at 4 °C and 10,000 rpm for 10 min. The upper methanol water phase was placed in the nitrogen blowing instrument (NBI, HSC-24B, Tianjin Hengao Technology Development Co. Ltd, Tianjin, China) to blow off the methanol, and then the supernatants were freeze-dried, and then stored under −80°C until NMR analysis [11].

In the NMR measurements, the samples were dissolved in 550 mL 99.8% D_2O phosphate buffer (0.2 M, pH = 7.0), which contained 0.05% (w/v) 3-(trimethylsilyl) sodium propionate -2, 2, 3, 3-d4 (TSP). After rotating for 15 s and centrifuging for 10 min at 12,000 rpm and 4 °C, the supernatant was

Preprints (www.preprints.org) | NOT PEER-REVIEWED | Posted: 24 May 2019 doi:10.20944/preprints201905.0301.v1

Peer-reviewed version available at Appl. Sci. 2019, 9, 2240; doi:10.3390/app9112240

transferred to a clean nuclear magnetic resonance tube (5 mm) for analysis. The ^{1}H-NMR spectrum was recorded in the 298 K at 500 MHz nuclear magnetic resonance spectroscopy (Bruker Avance III, Bruker Instruments, Darmstadt, Germany). Field-frequency locking with D_2O and TSP was used as a reference for chemical shift (1H, D 0.00). The carrpurcell-meiboom-gill sequence [90 (t-180-t) n-acquisition], which is edited by lateral relaxation, has a total spin-echo delay (2 n t) of 40 ms. The spectra were recorded in 64K data points with 128 scans, ranging from −5–15 ppm. By multiplying FIDS with exponential weighting function (corresponding to line broadening at 0.5Hz), Fourier transform was performed on the spectrum.

2.6. Spectral Pre-Processing and Data Analysis

All ^{1}H NMR spectra were phase and baseline corrections, and the peak was manually calibrated using Topspin software (Bruker BioSpin GmbH, version 3.5, Rheinstetten, Karlsruhe, Germany). Then the peak was exported to ASCII file using Mestrec (version 4.9.6, Mestrelab Research SL, Santiago de Compostela, Spain) and imported into R software (https://www.r-project.org/) for further analysis. The region containing residual water signal was removed. The spectrum was combined with an adaptive intelligent algorithm. Before multivariate data analysis, the remaining trash cans were the probability quotient normalization and Pareto scale.

Orthogonal signal correction partial least squares discriminant analysis (OSC-PLS-DA) was used to reveal the metabolic differences among groups. Score charts are used to show clustering between categories, and load/s charts are used to identify different metabolites between two groups. Differential metabolites are metabolites in the upper right quadrant and the lower left quadrant of the S diagram. According to the correlation coefficient from blue to red, the loading graph is color coded. The model was validated internally by repeated two cross-validations and externally by a permutation test.

2.7. Statistical Analysis

Data on the inhibitory effects of carvacrol on mycelial growth, mycelial weights, and water-retention rate were analyzed by variance analysis (ANOVA) using the SPSS version 17.0 (SPSS Inc., Chicago, IL, USA). The significant difference of means was performed with the Duncan's test at $p < 0.05$.

3. Results

3.1. Effects of Carvacrol on P. Digitatum *Mycelial Growth on PDA*

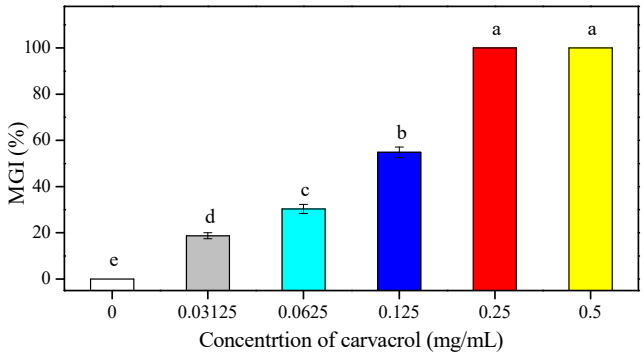

Figure 1. The antifungal efficacy of carvacrol on the in vivo mycelial growth inhibition (MGI) of *P. digitatum* on PDA. Bars indicate the mean ± standard deviation (S.D.) and those labeled with different letters (**a**, **b**, **c**, **d**, and **e**) were significantly different according to Duncan's test ($p < 0.05$).

The inhibitory effect of carvacrol on the growth of *P. digitatum* was quite obvious and a significant growth inhibition on PDA medium was seen in a dose-dependent manner ($p < 0.05$)

Preprints (www.preprints.org) | NOT PEER-REVIEWED | Posted: 24 May 2019 doi:10.20944/preprints201905.0301.v1

Peer-reviewed version available at Appl. Sci. 2019, 9, 2240; doi:10.3390/app9112240

(Figure 1). The increasing carvacrol concentrations had higher mycelial growth inhibition (MGI). As a whole, over one-fifth of the *P. digitatum* mycelial growth was inhibited at 0.0625 mg/mL of carvacrol, but 0.125 mg/mL concentration inhibited more than half (54.84%) of the mycelial growth. The higher carvacrol concentrations (0.25 and 0.5 mg/mL) completely inhibited the mycelial growth of *P. digitatum* (Figure 1).

Based on the observation of *P. digitatum* in mycelial growth on PDA medium with carvacrol treatments at 0, 0.03125, 0.0625, 0.125, 0.25, and 0.5 mg/mL during the incubation period at 25 °C, carvacrol treatments at the concentrations of 0.125 mg/mL and 0.25 mg/mL completely inhibited *P. digitatum* in mycelial growth at the 2nd day and 7th days of incubation, respectively. Therefore, the values of MIC and MFC were 0.125 mg/mL and 0.25 mg/mL, respectively (Figure 2).

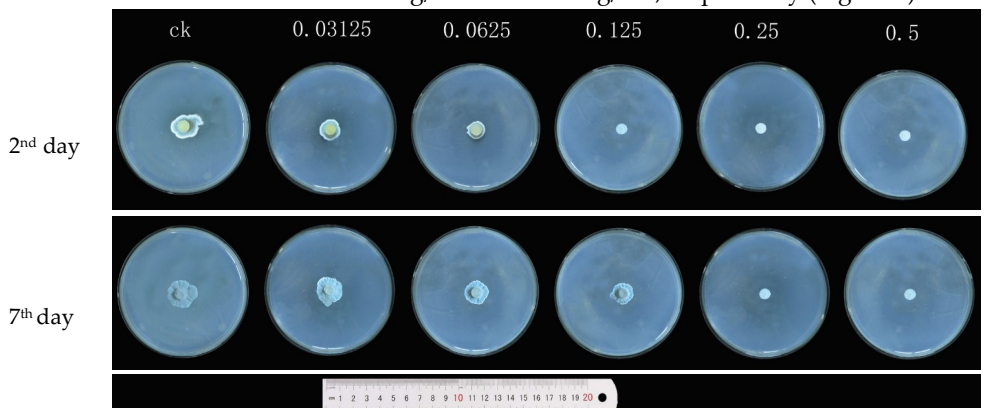

Figure 2. The effect of the growth diameter of *P. digitatum* treated with different concentrations of carvacrol (0, 0.03125, 0.0625, 0.125, 0.25, and 0.50 mg/mL) at 2 days and 7 days post-inoculation (dpi).

3.2. Effects of Carvacrol on Mycelial Weights in PDB

The mycelial weights of *P. digitatum* in carvacrol treatment and control groups are shown in Table 1. The data showed that mycelial growth biomass was strongly inhibited with increasing the carvacrol concentration. Initially, the wet and dry weights were 3.736 g and 0.393 g/100 mL at the lower carvacrol concentration of 0.0625 mg/mL, respectively. At higher carvacrol concentrations (0.125, 0.25 and 0.50 mg/mL), the effect on mycelial weights was recorded at a significant level ($p < 0.05$) in comparison with the control group.

Table 1. The mycelial weights and water-retention rate of *P. digitatum* treated with several concentrations of carvacrol.

Concentrations (mg/mL)	Mycelial Weight (g/100 mL)		Water-retention Rate (%)
	Wet Weight	Dry Weight	
0	4.868 ± 0.288 ^{a}	0.419 ± 0.011 ^{a}	91.38 ± 0.29 ^{a}
0.03125	4.487 ± 0.185 ^{a}	0.407 ± 0.008 ^{a}	90.89 ± 0.33 ^{a}
0.0625	3.736 ± 0.113 ^{b}	0.393 ± 0.015 ^{ab}	89.47 ± 0.48 ^{b}
0.125	3.065 ± 0.267 ^{c}	0.368 ± 0.016 ^{bc}	87.69 ± 0.77 ^{c}
0.25	2.895 ± 0.170 ^{c}	0.357 ± 0.012 ^{c}	87.57 ± 0.39 ^{c}
0.5	2.671 ± 0.232 ^{c}	0.345 ± 0.020 ^{c}	86.96 ± 0.65 ^{c}

Values are mean ± S.E. The data followed by different letters within the column are significantly different according to Duncan's test ($p < 0.05$).

3.3. Effect of Carvacrol *on Water-Retention Rate of P. Digitatum*

Water is the main component in the fungal cell and account for about 90% of mycelial fresh weight and plays an important role in regulating of cell osmotic pressure. The water-retention rate

Preprints (www.preprints.org) | NOT PEER-REVIEWED | Posted: 24 May 2019 doi:10.20944/preprints201905.0301.v1

Peer-reviewed version available at Appl. Sci. 2019, 9, 2240; doi:10.3390/app9112240

is used as an index of lipid peroxidation that is related to membrane damage leading to cell aging. The lower water-retention index shows higher membrane damages, and vice versa. The effect of carvacrol on the water-retention rate of *P. digitatum* mycelia is shown in Table 1. Different concentrations of carvacrol treatments were used to evaluate the mycelial membrane damage. The water-retention rate of *P. digitatum* mycelia was decreased and treated by carvacrol in a dose-dependent manner. The results demonstrate that the water-retention rate of *P. digitatum* mycelia was more significantly inhibited by the higher concentrations (0.125, 0.25, and 0.50 mg·mL^{-1}) of carvacrol.

3.4. Metabolites Identified in ^{1}H-NMR Spectra

The representative 500 MHz ^{1}H-NMR spectra of mycelia obtained from the control group and MIC carvacrol administration group are shown in Figure 3. Chemical shifts assignments of metabolites were shown in the supplementary material (Supplementary Table S1). Nuclear magnetic resonance (NMR) was allocated by searching publicly-accessible metabolome databases (such as the Human Metabonomics Database and Madison Qingdao Metabonomics Joint Database) based on chemical changes reported in the literature.

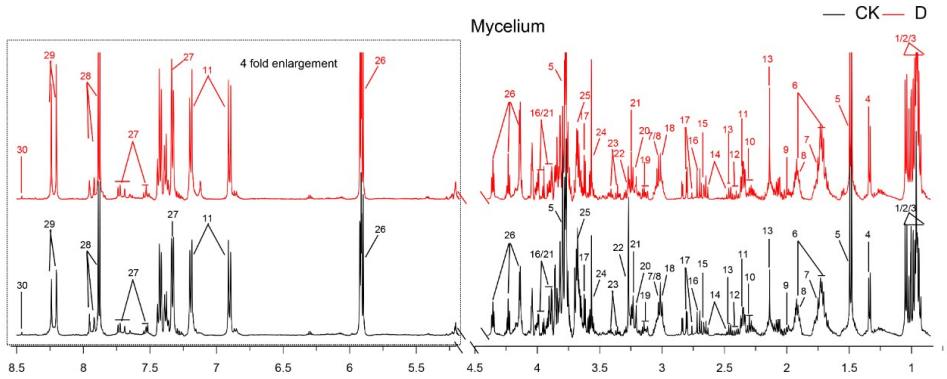

Figure 3. The typical 500 MHz CPMG ^{1}H-NMR spectra for 2 groups. Keys: 1. Isoleucine; 2. Leucine; 3. Valine; 4. Lactate; 5. Alanine; 6. Lysine; 7. Putrescine; 8. 4-Aminobutyrate; 9. Acetate; 10. Glutamate; 11. Acetaminophen; 12. Succinate; 13. Glutamine; 14. Glutathione; 15. 5,6-Dihydrouracil; 16. Aspartate; 17. Sarcosine; 18. Phenylalanine; 19. Ethanolamine; 20. Choline; 21. Betaine; 22. Arginine; 23. Methanol; 24. Glycine; 25. π-Methylhistidine; 26. Uracil; 27. Tryptophan; 28. Xanthine; 29. Adenine; 30. Formate.

3.5. Multivariate Analysis of ^{1}H-NMR Spectral Data

To evaluate the antifungal activity of carvacrol on *P. digitatum*, the OSC-PLS-DA model was constructed and all NMR data obtained from the control group (CK) and carvacrol administration group (D) at 4, 8 and 12 h were analyzed. In Figure 4 B–D, each point manifested a sample, and each clustering represented a corresponding metabolic pattern in different groups. Figure 4B shows that the two groups were not well separated at 4 h. However, with the passage of time, the control group and the drug group were separated further and further, and the CK and D groups were the furthest away in the scores plot at 12 h (Figure 4D). This result shows that the metabolomic changes in D group increased from 4 h to 12 h. At 12 h, the metabolic spectrum of group D changed fundamentally, reflecting the rapid response of the strain to carvacrol. The trajectory plot (Figure 4A) also exhibited a good separation between the CK and D groups, showing an apparent time-dependent antifungal activity of carvacrol on *P. digitatum*.

Preprints (www.preprints.org) | NOT PEER-REVIEWED | Posted: 24 May 2019 doi:10.20944/preprints201905.0301.v1

Peer-reviewed version available at Appl. Sci. 2019, 9, 2240; doi:10.3390/app9112240

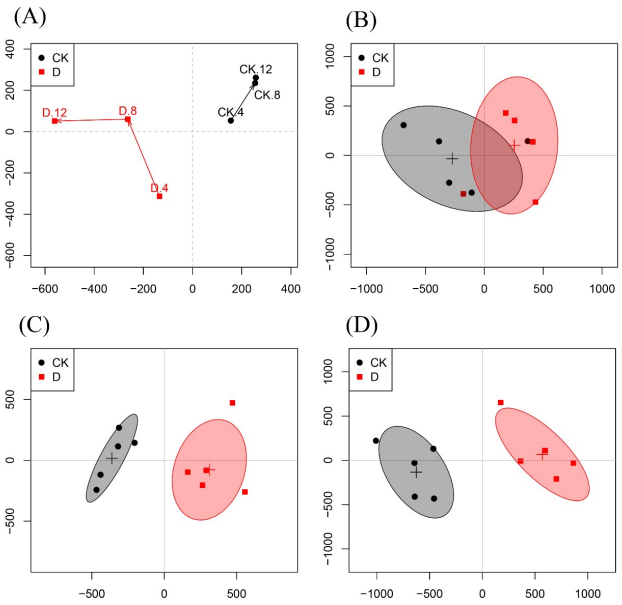

Figure 4. A: Score trajectory of the OSC-PLS-DA analysis in the CK group and D group at 4, 8, 12 h. **B, C, D:** Scores plots of CK and D groups at 4 h, 8 h, and 12 h, respectively.

In the 12 h S-plot (Figure 5B), different shapes and colors of the dots show different metabolites. The contribution of these metabolites to the group is related to their distance to the center; variables farther away from the center contribute more to the group separation. On the basis of the correlation coefficient, the 12-hours loading plots (Figure 5C,D) are coded with cold and warm tones, and the correlation increases gradually from blue to red. Significant decrease of lactate, alanine, glutamate, glutamine, glutathione, aspartate, sarcosine, phenylalanine, ethanolamine, choline, arginine, methanol, glycine, π-Methylhistidine and xanthine, and marked increase of leucine, uracil, tryptophan and adenine were found in the carvacrol dosed group.

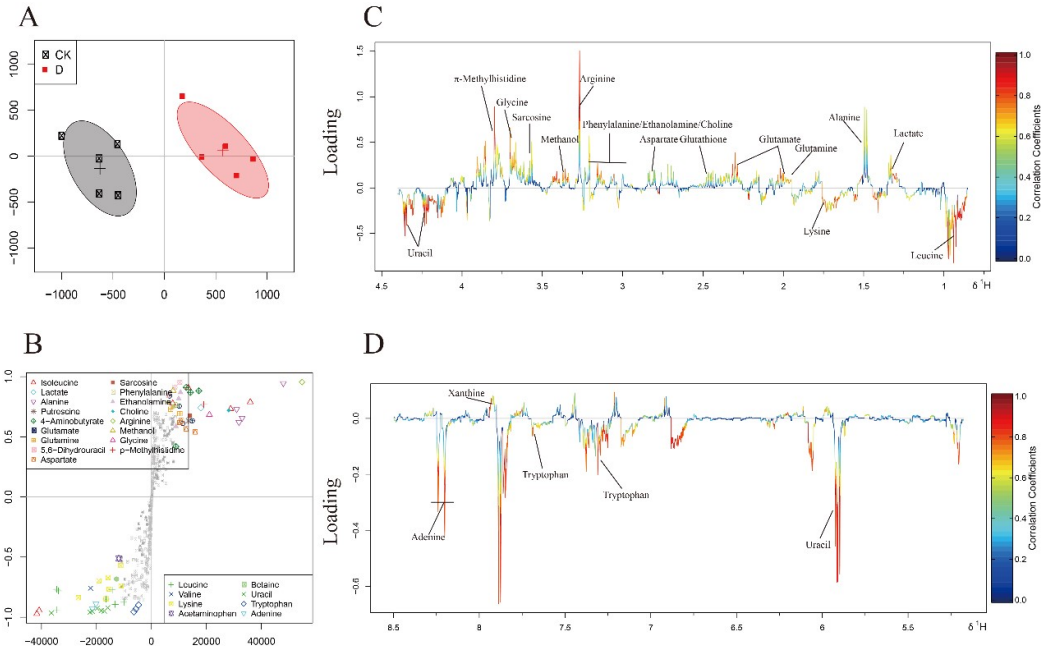

Figure 5. OSC-PLS-DA analysis of NMR data at 12 h. (**A**) The OSC-PLS-DA Score plot. (**B**) S-plot. (**C**, **D**) Color-coded loadings plots. The use of color bars, where red and blue represent metabolites, is

Preprints (www.preprints.org) | NOT PEER-REVIEWED | Posted: 24 May 2019 doi:10.20944/preprints201905.0301.v1

Peer-reviewed version available at Appl. Sci. 2019, 9, 2240; doi:10.3390/app9112240

statistically significant or insignificant in facilitating the separation of groups. In the CK group, the peak of the positive and negative states showed that the decrease and increase of metabolites were correlated with the score plot.

The results of the normality test of metabolites are shown in Table 2. The folding changes (FC) of metabolites and their associated P values were calculated and corrected in color tables. Collapse change values are color-coded after log conversion. Cell units were filled with red or blue to indicate the increase or decrease respectively of metabolites in the carvacrol-treated group compared with the control group.

Table 2. Differential expression of metabolites between two groups at 12 h.

No	Metabolites	D/CK	
		[a] FC	[b] P
1	Isoleucine	0.04	
2	Leucine	0.5	*
3	Valine	−0.11	
4	Lactate	−0.52	*
5	Alanine	−0.82	**
6	Lysine	0.25	
7	Putrescine	−0.18	
8	4-Aminobutyrate	−0.27	
9	Acetate	0.1	
10	Glutamate	−0.41	*
11	Acetaminophen	0.04	
12	Succinate	−0.26	
13	Glutamine	−1.17	***
14	Glutathione	−0.65	*
15	5-6-Dihydrouracil	−0.3	
16	Aspartate	−0.71	**
17	Sarcosine	−1.02	**
18	Phenylalanine	−1.65	***
19	Ethanolamine	−0.51	*
20	Choline	−1.51	***
21	Betaine	0.06	
22	Arginine	−1.86	***
23	Methanol	−0.75	**
24	Glycine	−1.09	**
25	π-Methylhistidine	−1	*
26	Uracil	1.13	**
27	Tryptophan	0.37	*
28	Xanthine	−1.42	***
29	Adenine	1.47	***
30	Formate	−0.07	

[a] FC: Color-coded according to the fold-change value; Color coded according to the $\log_2$(FC), red represents increased and blue represents decreased concentrations of metabolites. Color bar 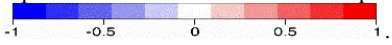

.

[b] *P* values corrected by Benjamini-Hochberg methods were calculated based on a parametric Student's t-test or a nonparametric Mann-Whitney test (dependent on the conformity to the normal distribution). * $p < 0.05$, ** $p < 0.01$, *** $p < 0.001$.

Preprints (www.preprints.org) | NOT PEER-REVIEWED | Posted: 24 May 2019 doi:10.20944/preprints201905.0301.v1

Peer-reviewed version available at Appl. Sci. 2019, 9, 2240; doi:10.3390/app9112240

4. Discussion

The current study comprehensively evaluated the antifungal activity of carvacrol against *P. digitatum* through ^{1}H-NMR metabonomics. Following the important metabolites selected by OSC-PLS-DA loading/S-diagram, METPA (http://www.metaboanalyst.ca) (Figure 6A) and KEGG (http://www.genome.jp/kegg/) were used for path analysis to determine biologically significant metabolic patterns and related pathways (Figure 6B–E).

Alanine, aspartate, glutamate, and glutathione metabolisms were imbalanced in the fungal hyphae (Figure 6). These metabolisms were also found in the correlation network of D group at 12 h. A strong positive correlation between aspartate, glutamate, alanine, and glutamine was seen, and a negative correlation between glutathione and lactate was also observed. These metabolic changes revealed that carvacrol induced the generation of heavy oxidative stress to disturb the energy and amino acid metabolism of *P. digitatum* (Supplementary Figure S1).

A significant decrease in the level of glutamate, glutamine, glycine and precursors of glutathione was observed in the D group. As an ROS scavenger, the level of glutathione also markedly decreased in the D group. Glutathione being endogenously expressed antioxidant enzyme that played an important role in the protection of cells against ROS by quickly eliminating free radicals [24]. Glutathione was consumed in large quantities in fungi against carvacrol-induced ROS. To sustain a certain level of glutathione in fungus, the synthesis of glutathione from glutamate, glutamine and glycine has to be enhanced [25], which will lead to the degradation of glutamate and glycine. In addition, a heavy load of ROS could enhance peroxidation of membrane lipids, leading to damage the cellular membranes [26]. The decreased level of choline and ethanolamine were seen in the D group compared with the CK group, and both are considered as the key players in the stability and integrity of cell membranes [27]. Therefore, any decrease in choline and ethanolamine may be due to excessive utilization for repairing the damaged membranes caused by ROS which are indicators of decreased level of sarcosine in D group [28]. In the current study, the sarcosine level in group D was lower than that in group CK, and was linked with the decrease of choline and glycine levels. These results reflect the disturbance of ROS to the sarcosine pathway caused by carvacrol.

The self-protection mechanism of fungus made it consume huge amounts of energy to avoid ROS mediated stress and repair the cell membranes. In order to produce more ATPs, the aerobic respiration in fungal hypha was enhanced while the glycolysis pathway was checked to a great extent. Such reduction in glycolysis was supported by the decreased level of lactate in D group. In addition, a marked decrease in phenylalanine, alanine, aspartate, and arginine levels was observed in D group. The glycogenic amino acids underwent degradation [29] and reflected an enhancement in the gluconeogenesis pathway that compensates the deficiency of glucose. The results further suggested that carvacrol helps produce energy and amino acid metabolic disorders in *P. digitatum*.

A significant increase in the transcriptional initiators e.g., uracil and adenine were found in the D group compared with the CK group (Table 2) [30]. The increased level of uracil and adenine revealed that carvacrol caused RNA damage to *P. digitatum*.

In this pioneering study, the antifungal activity of carvacrol against *P. digitatum* was studied by using the metabolomics approach based on ^{1}H-NMR. Carvacrol can cause an abnormal metabolic state of *P. digitatum* by interfering with different metabolic pathways such as energy and amino acid metabolisms. Furthermore, carvacrol could also induce damage to the RNA molecules and ROS production. Metabolomics provide a powerful and feasible tool for evaluating antifungal activity and exploring its potential mechanism.

Preprints (www.preprints.org) | NOT PEER-REVIEWED | Posted: 24 May 2019 doi:10.20944/preprints201905.0301.v1

Peer-reviewed version available at Appl. Sci. 2019, 9, 2240; doi:10.3390/app9112240

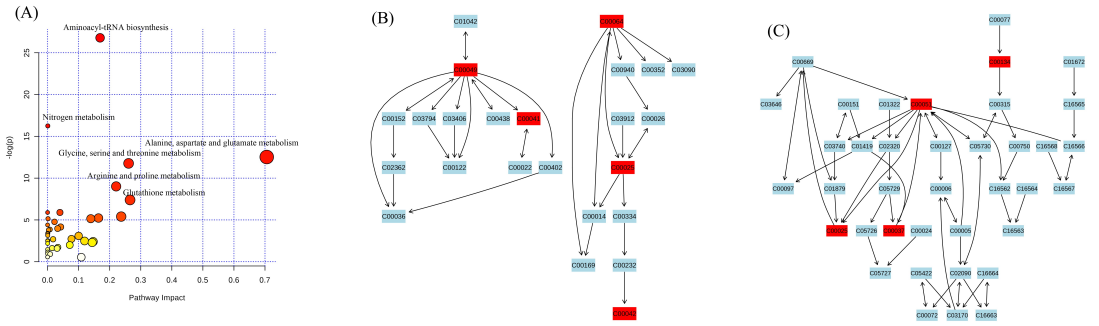

Figure 6. (**A**) In this study, metabolic analysis was used to analyze the pathway topology related to antifungal activity. The term "log p" is the conversion of the original p value calculated from enrichment analysis, and "impact" is the path impact value calculated from the path topology analysis. The bubble area is proportional to the effect of each path, and the color indicates the importance from the highest red to the lowest white. (**B**) Alanine, aspartate, glutamate metabolism; (**C**) glutathione metabolism.

Supplementary Material: Table S1: Chemical shifts assignment of metabolites, Figure S1: Correlation network analysis of D group at 12 h.

Author Contributions: conceptualization, C.W. and J.C.; methodology, C.W. and C.C.; formal analysis, C.W. and C.C.; investigation, Y.S.; W.Q. and C.C.; data curation, C.C.; writing—original draft preparation, C.W.; Y.S.; W.Q. and C.C.; writing—review and editing, C.W. and M. N.; supervision, C.W.; project administration, C.W. and C.C.; funding acquisition, J.C.

Funding: This research was funded by National Natural Science Foundation of China (NO.31760598) and Advantage Innovation Team Project of Jiangxi Province (NO.20181BCB24005).

Conflicts of Interest: The authors declare no conflict of interest.

References

1. Nicosia, M. G. L. D.; Pangallo, S.; Raphael, G.; Romeo, F. V.; Strano, M. C.; Rapisarda, P.; Droby, S.; Schena. Control of postharvest fungal rots on citrus fruit and sweet cherries using a pomegranate peel extract. *Postharvest Biol. Technol*. **2016**, *114*, 54-61.
2. Chen, J.; Shen, Y.; Chen, C.; Wan, C. Inhibition of key citrus postharvest fungal strains by plant extracts in vitro and *in vivo*: A review. *Plants* (Basel, Switzerland), **2019,** *8*, 26
3. Chen, C.; Cai, N.; Chen, J.; Peng, X.; Wan, C. Chitosan-Based Coating Enriched with Hairy Fig (*Ficus hirta* Vahl.) Fruit Extract for "Newhall" Navel Orange Preservation. *Coatings*, **2018**, *8*, 445.
4. Zafar, I.; Zora, S.; Ravjit, K.; Saeed, A. Management of citrus blue and green moulds through application of organic elicitors. *Australas. Plant Path*. **2012**, *41*, 69-77.
5. Hao, W.; Li, H.; Hu, M.Y.; Liu, Y.; Rizwan-ul-Haq, M. Integrated control of citrus green and blue mold and sour rot by *Bacillus amyloliquefaciens* incombination with tea saponin. *Postharvest Biol. Technol*. **2011**, *59*, 316–323.
6. Palou, L., Ali, L., Fallik, E., Romanazzi, G. GRAS, plant- and animal-derived compounds as alternatives to conventional fungicides for the control of postharvest dieseases of fresh horticultural produce. *Postharvest Biol. Technol*. **2016**, *122*, 41-52.
7. Gong, T., Li, C., Bian, B., Wu, Y., Dawuda, M. M., Liao, W. Advances in application of small molecule compounds for extending the shelf life of perishable horticultural products: A review. *Sci. Hort*. **2018**, *230*, 25-34
8. Zhang, M., Xu, L., Zhang, L., Guo, Y., Qi, X., He, L. Effects of quercetin on postharvest blue mold control in kiwifruit. *Sci. Hort*. **2018**, 228, 18-25
9. Ncama, K., Magwaza, L. S., Mditshwa, A., Tesfay, S. Z. Plant-based edible coatings for managing postharvest quality of fresh horticultural produce: A review. *Food Packaging Shelf* **2018**, *16*, 157-167
10. Zhang, X.F.; Guo, Y.J.; Guo, L.Y.; Jiang, H.; Ji, Q.H. In Vitro Evaluation of Antioxidant and Antimicrobial Activities of *Melaleuca alternifolia* Essential Oil. *Biomed. Res. Int*. **2018**, *2018*, 2396109.

Preprints (www.preprints.org) | NOT PEER-REVIEWED | Posted: 24 May 2019 doi:10.20944/preprints201905.0301.v1

Peer-reviewed version available at Appl. Sci. 2019, 9, 2240; doi:10.3390/app9112240

11. Wan, C.P.; Pei, L.; Chen, C.Y.; Peng, X.; Li, M.X.; Chen, M.; Wang, J.S.; Chen, J.Y. Antifungal Activity of *Ramulus cinnamomi* Explored by ^{1}H-NMR Based Metabolomics Approach. *Molecules* **2017**, *22*, 2237.
12. Trabelsi, D.; Hamdane, A.M.; Said, M.B.; Abdrrsbba, M. Chemical composition and antifungal activity of essential oils from flowers, leaves and peels of Tunisian *Citrus aurantium* against *Penicillium digitatum* and *Penicillium italicum*. *J. Essent. Oil Bear. Plants* **2016**, *19*, 1660–1674.
13. Can Baser, K.H. Biological and pharmacological activities of carvacrol and carvacrol bearing essential oils. *Curr. Pharma. Design*, **2008**, 14, 3106-3119.
14. Zotti, M., Colaianna, M., Morgese, M., Tucci, P., Schiavone, S., Avato, P., Trabace, L. Carvacrol: from ancient flavoring to neuromodulatory agent. *Molecules*, **2013**, 18, 6161-6172.
15. Pérez-Alfonso, C.O.; Martínez-Romero, D.; Zapata, P.J.; Serrano, M.; Valero, D.; Castillo, S. The effects of essential oils carvacrol and thymol on growth of *Penicillium digitatum* and *P. italicum* involved in lemon decay. *Int. J. Food Microbiol*. **2012**, *158*, 101–106.
16. Boubaker, H.; Karim, H.; Hamdaoui, A.E.; Msanda, F.; Leach, D.; Bombarda, I.; Vanloot, P.; Abbad, A.; Boudyach, E.H.; Aoumar, A.B. Chemical characterization and antifungal activities of four *Thymus* species essential oils against postharvest fungal pathogens of citrus. *Ind. Crop. Prod*. **2016**, *86*, 95–101.
17. Sun, X.; Narciso, J.; Wang, Z.; Ference, C.; Bai, J.; Zhou, K. Effects of chitosan-essential oil coatings on safety and quality of fresh blueberries. *J. Food Sci*. **2014**, *79*, M955-M960.
18. Keun, H. C.; Ebbels, T. M.; Antti, H.; Bollard, M. E.; Beckonert, O.; Schlotterbeck, G.; Senn, H.; Niederhauser, U.; Holmes, E.; Lindon, J. C.; Nicholson, J. K. Analytical Reproducibility in ^{1}H NMR-Based Metabonomic Urinalysis. *Chem. Res. Toxicol.* **2002**, *15*, 1380-1386.
19. Liu, X.; Zhang, L.; You, L.; Cong, M.; Zhao, J.; Wu, H.; Li, C.; Liu, D.; Yu, J. Toxicological responses to acute mercury exposure for three species of Manila clam *Ruditapes philippinarum* by NMR-based metabolomics. *Environ. Toxicol. Phar*. **2011**, *31*, 323-332.
20. Liu, Q., Wu, J. E., Lim, Z. Y., Aggarwal, A., Yang, H., Wang, S. Evaluation of the metabolic response of Escherichia coli to electrolysed water by ^{1}H NMR spectroscopy. *LWT-Food Sci. Technol*., **2017,** *79*, 428-436.
21. Picone, G., Laghi, L., Gardini, F., Lanciotti, R., Siroli, L., Capozzi, F. Evaluation of the effect of carvacrol on the *Escherichia coli* 555 metabolome by using ^{1}H-NMR spectroscopy. *Food Chem*., **2013**, *141*, 4367-4374.
22. Chen, C.; Qi, W.; Peng, X.; Chen, J.; Wan, C. Inhibitory Effect of 7-Demethoxytylophorine on *Penicillium italicum* and its Possible Mechanism. *Microorganisms* **2019**, 7, 36.
23. Tian, J.; Wang, Y.; Zeng, H.; Li, Z.; Zhang, P.; Tessema, A.; Peng, X. Efficacy and possible mechanisms of perillaldehyde in control of *Aspergillus niger* causing grape decay. *Int. J. Food Microbiol*. **2015**, *202*, 27-34.
24. Chen, C.; Fu, Y. H.; Li, M.H.; Li, M. H.; Ruan, L. Y.; Xu, H.; Chen, J. F.; Wang, J. S. Nuclear magnetic resonance-based metabolomics approach to evaluate preventive and therapeutic effects of *Gastrodia elata* Blume on chronic atrophic gastritis. *J. Pharmaceut. Biomed*. **2019**, *164*, 231-240.
25. Ballatori, N.; Jacob, R.; Boyer J.L. Intrabiliary glutathione hydrolysis. A source of glutamate in bile. *J. Bio. Chem*. **1986**, *261*, 7860-7865.
26. Apel, K.; Hirt, H. Reactive oxygen Species: Metabolism, Oxidative Stress, and Signal Transduction. *Annu. Rev. Plant Biol*. **2004**, *55*, 373-399.
27. Fu, Y.; Si, Z.; Li, P.; Li, M.; Zhao, H.; Jiang, L.; Xing, Y.; Hong, W.; Ruan, L.; Wang, J. S. Acute psychoactive and toxic effects of D. metel on mice explained by ^{1}H NMR based metabolomics approach. *Metab. Brain Dis*. **2017**, *32*, 1295-1309.
28. Boncompagni, E.; Østerås, M.; Poggi, M. C.; le Rudulier, D. Occurrence of Choline and Glycine Betaine Uptake and Metabolism in the Family Rhizobiaceae and Their Roles in Osmoprotection. *Appl. Environ. Microb*. **1999**, *65*, 2072-2077.
29. Armstrong, C. W.; McGregor, N. R.; Sheedy, J. R.; Buttfield, I.; Butt, H. L.; Gooley, P. R. NMR metabolic profiling of serum identifies amino acid disturbances in chronic fatigue syndrome. *Clinica Chimica Acta*. **2012**, *413*, 1525-1531.
30. And, K.S.; Shinkai, S. Molecular Recognition of Adenine, Cytosine, and Uracil in a Single-Stranded RNA by a Natural Polysaccharide: Schizophyllan. *Toxicol. Lett*. **2000**, *122*, 1-8.